Andreev nanoprobe of half-metallic CrO_2 films using superconducting cuprate tips

C. S. Turel,[1] I. J. Guilaran,[2] P. Xiong,[3] and J. Y. T. Wei[1,4,a)]
[1]*Department of Physics, University of Toronto, 60 St. George Street, Toronto, Ontario M5S1A7, Canada*
[2]*Department of Physics, Union University, Jackson, Tennessee 38305, USA*
[3]*Department of Physics, Florida State University, Tallahassee, Florida 32306, USA*
[4]*Canadian Institute for Advanced Research, Toronto, Ontario M5G1Z8, Canada*

(Received 8 August 2011; accepted 4 October 2011; published online 9 November 2011)

Superconducting tips of $YBa_2Cu_3O_{7-x}$ were used to perform point-contact Andreev reflection spectroscopy on half-metallic CrO_2 thin films. At 4.2 K, strong suppression of the *d*-wave Andreev reflection characteristics was observed, consistent with the high spin polarization of CrO_2. Our technique was validated by comparison with data taken on non-magnetic Au films and with data taken by superconducting Pb tips. The point contacts were estimated to be $\lesssim$10 nm in size, attesting to their ballistic and microscopic nature. Our results demonstrate the feasibility of using superconducting cuprate tips as spin-sensitive nanoprobes of ferromagnets. © *2011 American Institute of Physics*. [doi:10.1063/1.3659411]

Andreev reflection (AR) is the process by which an electron incident from a normal metal (N) is converted into a Cooper pair in a superconductor (S).[1] In the case of *s*-wave pairing, AR is sensitive to the electron spin polarization in the metal counterelectrode, as a direct consequence of spin conservation.[2] For a normal metal, where there is an equal density of spin-up versus spin-down states at the Fermi level E_f, a spin-up electron can be retroreflected as a spin-down hole to form a spin-singlet pair thus doubling the conductance across the NS junction. For a half metal, where the electrons at E_f are 100% spin-polarized, such retroreflection is inhibited thus suppressing the enhancement of junction conductance. This inherent spin sensitivity of AR has been exploited to determine the spin polarization in a variety of itinerant ferromagnets by measuring the conductance spectra of both point contact and fixed planar junctions.[3,4]

In the case of superconductors with *d*-wave pairing, AR can also involve quasiparticle interference and result in the formation of zero-energy bound states at the NS interface. Basically, because of the order-parameter sign change across *d*-wave line nodes, consecutively Andreev-reflected quasiparticles can constructively interfere to produce a zero-bias peak (ZBP) in the conductance spectrum on non-principal axis junctions.[5,6] Since AR is inherently spin-dependent, this ZBP is expected to be suppressed for a ferromagnetic counterelectrode depending on the extent of its spin polarization.[7,8,10] Such ZBP suppression effect has been previously studied in fixed planar junctions for high-T_c cuprate superconductors[11,12] but never in point contact junctions.

In this letter we used superconducting tips of $YBa_2Cu_3O_{7-x}$ (YBCO) to perform point contact spectroscopy on ferromagnetic thin films of CrO_2 in order to study how the *d*-wave AR characteristics on YBCO are affected by the electron spin polarization of CrO_2. While YBCO is known to have a predominantly *d*-wave pairing symmetry,[13] CrO_2 is believed to be an exemplary half-metal, with nearly perfect spin polarization.[14] In order to validate our technique and interpretation, we compared conductance spectra measured on YBCO/CrO_2 junctions with spectra taken on YBCO/Au and Pb/CrO_2 junctions. Spectra with ZBPs were observed on YBCO/Au, while spectra with zero-bias dips (ZBD) were observed on YBCO/CrO_2 and Pb/CrO_2. These observations provide direct evidence for the suppression of *d*-wave Andreev states by spin polarization in point-contact junctions. Our point-contact radius was estimated to be $\approx$0.7–6.0 nm, demonstrating that superconducting cuprate tips can potentially be used to probe electron spin polarization by AR spectroscopy at the nanoscale.

Epitaxial thin film samples of CrO_2, $\approx$200–250 nm thick, were fabricated on (100)-oriented TiO_2 substrates using a chemical vapor deposition growth technique.[15–19] To gauge the half metallicity of our CrO_2 film surfaces, Pb tips were used as a conventional *s*-wave superconductor for measuring the spin polarization of our films by *s*-wave AR. Measurements were made in a ^{4}He dipper probe between 4.2 and 8.5 K. Differential conductance dI/dV versus voltage V spectra were obtained using a four-point geometry with standard ac lock-in technique. The CrO_2 films we measured had resistances much smaller than the point-contact resistances, thus ruling out any issues of spreading resistance.[20]

Figure 1 shows temperature evolution of the dI/dV spectra measured on a Pb/CrO_2 point-contact junction. The spectrum at each temperature was normalized relative to the dI/dV taken at energies higher than Δ^{Pb}, the superconducting energy gap of Pb. At 7.5 K, above the T_c of Pb, the dI/dV spectrum shows negligible dependence on V. As temperature is lowered below T_c, the subgap dI/dV is progressively suppressed. The spectral data is fitted to the modified Blonder-Tinkham-Klapwijk (BTK) model accounting for barrier strength Z and spin polarization P.[21,22,29,30] The parameters used in the fit shown in Fig. 1 are $\Delta^{Pb} = 0.95$ meV, $Z = 1.2$, and $P = 0.85$. This large spin polarization is consistent with previous point-contact measurements of CrO_2,[3,23] even though our P value is slightly smaller as can be explained by our relatively larger Z.[20,23]

Having confirmed the near-half metallicity of our CrO_2 films using *s*-wave superconducting tips, the effect of spin

a)Electronic mail: wei@physics.utoronto.ca.

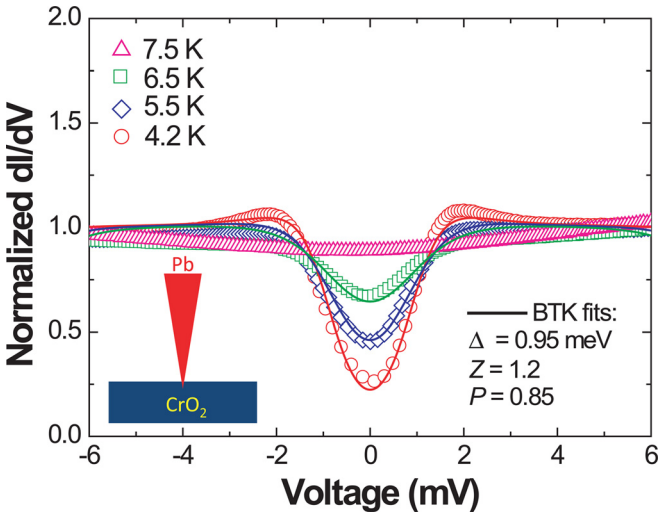

FIG. 1. (Color online) Normalized differential conductance versus bias voltage spectrum taken on a Pb/CrO_2 point-contact junction at different temperatures. Open symbols correspond to the spectral data, and solid lines are fits using the BTK model.

polarization on *d*-wave Andreev states can be determined by measuring YBCO/CrO_2 junctions. YBCO tips were fabricated by cutting slivers, typically $2 \times 2 \times 5$ mm^3, from a YBCO crystal monolith grown in a melt-zone furnace. The YBCO slivers were mechanically polished into a fine tip, nominally pointed along the (110) axis. After ultrasonic cleaning in ethanol, the YBCO tips were re-annealed at 500 °C in flowing oxygen for 36 h. Before measuring YBCO/CrO_2 junctions, the YBCO tips were tested on normal-metal Au films to ensure that ZBPs due to *d*-wave Andreev interference were observed in the *dI*/*dV* spectrum. Several YBCO tips were used for the Au/YBCO point-contact junctions, whose resistance ranged from ≈10 to 500 Ω at 4.2 K.

Figure 2 shows the normalized *dI*/*dV* spectrum measured on a typical Au/YBCO point-contact junction at 4.2 K, and the unnormalized data are shown in the top right inset. The *dI*/*dV* data were normalized by dividing out, using a polynomial fit, the spectral background which is often

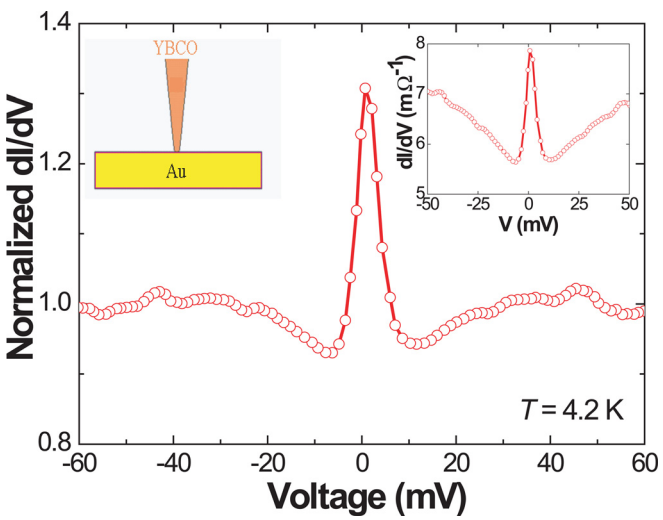

FIG. 2. (Color online) Normalized conductance spectrum measured on a Au film using a YBCO tip at 4.2 K. Right inset is a plot of the unnormalized spectrum showing the linear background which is characteristic of YBCO.

observed in YBCO junctions.[24,25] In the normalized spectrum, a pronounced ZBP is present along with a gap-like structure within $\sim \pm 20$ mV, which is consistent with the superconducting energy-gap maximum of optimally doped YBCO.[26] Such ZBP structures have been commonly observed on YBCO for non-principal axes junctions and attributed to *d*-wave Andreev interference.[26,27]

Figure 3 shows the normalized *dI*/*dV* spectrum measured on a typical YBCO/CrO_2 film junction at 4.2 K, and the unnormalized data are shown in the top right inset. The *dI*/*dV* data were normalized by fitting the spectral background beyond ± 20 mV to a polynomial and dividing the entire spectrum by the fit. For $|V| \lesssim 20$ mV, the normalized *dI*/*dV* is relatively independent of voltage. For $|V| \gtrsim 20$ mV, a ZBD is clearly observed. Noticeable in both the normalized and unnormalized spectra are spectral kinks at ± 22 mV, where the slope of *dI*/*dV* shows an inflection, as indicated by the arrows in the inset. The position of these kinks can be related to Δ_0 the superconducting gap maximum of optimally doped YBCO, signaling a crossover into the subgap regime where *dI*/*dV* becomes suppressed by the spin polarization of CrO_2.

To confirm that the ZBD observed in the *dI*/*dV* spectrum at 4.2 K is due to the spin-polarization of CrO_2 and not to the spectral background of YBCO, we also measured YBCO/CrO_2 junction at 100 K, above the T_c of YBCO. This normal-state data is plotted in the top left inset of Fig. 3 and can be compared with the 4.2 K data shown in the top right inset. At 100 K, YBCO is not superconducting, and the *dI*/*dV* spectrum, which does not show the kinks observed at 4.2 K, can be fitted over the entire voltage range using a polynomial. At 4.2 K, a similar polynomial can only fit the spectral regime for $e|V| > \Delta_0$. For $e|V| < \Delta_0$, the measured *dI*/*dV* deviates from the fit to the spectral background, indicating that the ZBD is in fact due to subgap spectral suppression.

It is worth noting that the YBCO/CrO_2 junction resistance at 4.2 K ranged from 100 to 4000 Ω. A high junction

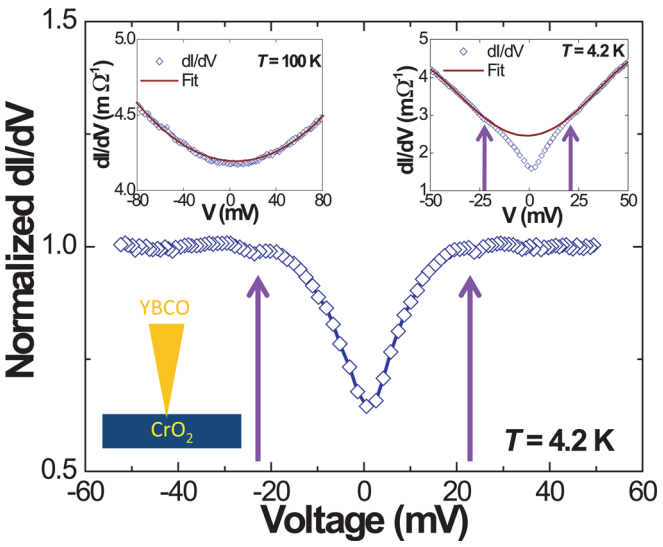

FIG. 3. (Color online) Normalized conductance spectrum measured on a CrO_2 film using a YBCO tip at 4.2 K. Insets show the unnormalized differential conductance spectra taken at 4.2 K (right) and at 100 K (left). Open symbols represent the data while solid lines are a polynomial fit to the background. Arrows indicate spectral kinks, whose locations are consistent with the superconducting gap maximum for YBCO.

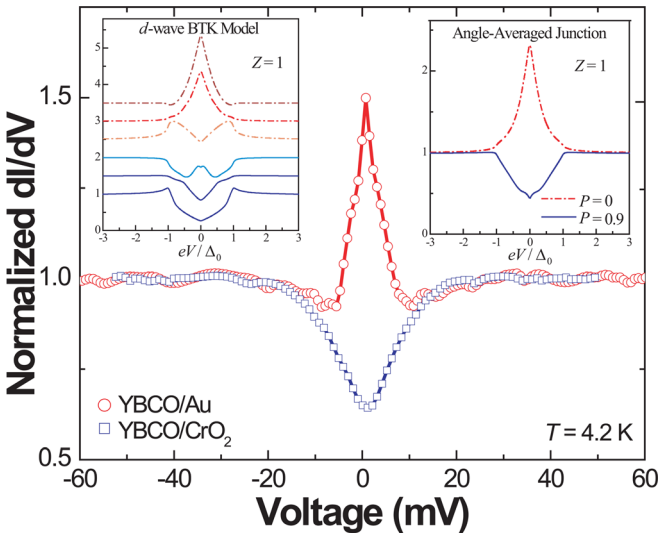

FIG. 4. (Color online) Comparison of the normalized conductance spectra taken on YBCO/Au (circles) and YBCO/CrO_2 (squares) at 4.2 K. Left inset shows various spectra calculated using the spin-dependent *d*-wave BTK model, for three junctions oriented normal to the *ab*-plane at $Z=1$: upper three curves are for $P=0$, with the junction normal rotated by 0, $\pi/12$ and $\pi/4$ (top to bottom) from the *d*-wave node axis; the lower three curves are for $P=0.9$ at the same three junction angles. Right inset shows two angle-averaged spectra ($P=0$ for upper, $P=0.9$ for lower), each averaged within a Gaussian envelope of width $\pi/6$ about the *d*-wave node axis, to simulate our nominally-oriented (110) YBCO tip junctions.

resistance R indicates a small contact area, implying that the electron transport across the interface is highly local. The effective point-contact radius a can be calculated using the Wexler formula,[28] $R \approx 4\rho l/3\pi a^2 + \rho/2\,a$, where ρ is the residual resistivity and l is the mean free path. Using $\rho \approx 50\,\mu\Omega\,\mathrm{cm}$ and $l \approx 10\,\mathrm{nm}$ for YBCO (Ref. 26) and $R \approx 0.1 - 4\,\mathrm{k}\,\Omega$, our point contact radius was estimated to range from $a \approx 0.7$–$6.0\,\mathrm{nm}$, attesting to their ballistic ($a < l$) and microscopic nature. Such small size of our YBCO point contacts suggests that they may be used to measure the spin polarization of individual magnetic domains.

To more clearly visualize the effect of spin polarization on YBCO point contacts, we compare the normalized dI/dV spectrum taken on YBCO/CrO_2 from Fig. 3 with a spectrum taken on YBCO/Au, as shown in Fig. 4. For $e|V| > \Delta_0$ both spectra are relatively featureless. For $e|V| < \Delta_0$ YBCO/Au shows a pronounced ZBP while YBCO/CrO_2 shows a distinct ZBD, with noticeable dips and kinks near Δ_0. To interpret these results more quantitatively, we performed spectral simulations using the spin-dependent *d*-wave BTK theory, as given by Refs. 7–10. The left inset shows several dI/dV spectra for various "in-plane" junction orientations and two values of P at a fixed Z, illustrating the spectral variety for ideally oriented junctions. The right inset shows the two corresponding angle-averaged spectra, each averaged within an Gaussian envelope centered on the *d*-wave node axis, to simulate our nominally oriented (110) YBCO tip junctions. There is good spectral resemblance between the YBCO/Au data and the $P=0$ simulation and between the YBCO/CrO_2 data and the $P=0.9$ simulation. These results confirm that the ZBP structure, which is formed by *d*-wave Andreev interference, is indeed suppressed by the high spin polarization of CrO_2 in our YBCO point-contact spectra.

This work was supported by NSERC, CFI-OIT and the Canadian Institute for Advanced Research. We thank Y.-T. Yen for technical assistance.

[1]G. E. Blonder, M. Tinkham, and T. M. Klapwijk, Phys. Rev. B **25**, 4515 (1982).
[2]M. J. M. de Jong and C. W. J. Beenakker, Phys. Rev. Lett. **74**, 1657 (1995).
[3]R. J. Soulen, Jr., J. M. Byers, M. S. Osofsky, B. Nadgorny, T. Ambrose, S. F. Cheng, P. R. Broussard, C. T. Tanaka, J. Nowak, J. S. Moodera, A. Barry, and J. M. D. Coey, Science **282**, 85 (1998).
[4]S. K. Upadhyay, A. Palanisami, R. N. Louie, and R. A. Buhrman, Phys. Rev. Lett. **81**, 3247 (1998).
[5]C.-R. Hu, Phys. Rev. Lett. **72**, 1526 (1994).
[6]Y. Tanaka and S. Kashiwaya, Phys. Rev. Lett. **74**, 3451 (1995).
[7]S. Kashiwaya, Y. Tanaka, N. Yoshida, and M. R. Beasley, Phys. Rev. B **60**, 3572 (1999).
[8]I. Zutic and O. Valls, Phys. Rev. B **60**, 6320 (1999).
[9]J.-X. Zhu, B. Friedman, and C. S. Ting, Phys. Rev. B **59**, 9558 (1999).
[10]I. Zutic and O. Valls, Phys. Rev. B **61**, 1555 (2000).
[11]V. A. Vas'ko, K. R. Nikolaev, V. A. Larkin, P. A. Kraus, and A. M. Goldman, Appl. Phys. Lett. **73**, 844 (1998).
[12]Z. Y. Chen, A. Biswas, I. Zutic, T. Wu, S. B. Ogale, R. L. Greene, and T. Venkatesan, Phys. Rev. B **63**, 212508 (2001).
[13]C. C. Tsuei and J. R. Kirtley, Rev. Mod. Phys. **72**, 969 (2000).
[14]J. S. Parker, S. M. Watts, P. G. Ivanov, and P. Xiong, Phys. Rev. Lett. **88**, 196601 (2002).
[15]L. Ranno, A. Barry, and J. M. D. Coey, J. Appl. Phys. **81**, 5774 (1997).
[16]X. W. Li, A. Gupta, T. R. McGuire, P. R. Duncombe, and G. Xiao, J. Appl. Phys. **85**, 5585 (1999).
[17]A. Gupta, X. W. Li, S. Guha, and G. Xiao, Appl. Phys. Lett. **75**, 2996 (1999).
[18]P. G. Ivanov, S. M. Watts, and D. M. Lind, J. Appl. Phys. **89**, 1035 (2001).
[19]A. Anguelouch, A. Gupta, G. Xiao, G. X. Miao, D. W. Abraham, S. Ingvarsson, Y. Ji, and C. L. Chien, J. Appl. Phys. **91**, 7140 (2002).
[20]G. T. Woods, R. J. Soulen, Jr., I. Mazin, B. Nadgorny, M. S. Osofsky, J. Sanders, H. Srikanth, W. F. Egelhoff, and R. Datla, Phys. Rev. B **70**, 054416 (2004).
[21]G. J. Strijkers, Y. Ji, F. Y. Yang, C. L. Chien, and J. M. Byers, Phys. Rev. B **63**, 104510 (2001).
[22]We note that the BTK model used here largely neglects the Andreev evanescent wave, which could result in a small systematic correction to the calculated spectra.
[23]Y. Ji, G. J. Strijkers, F. Y. Yang, and C. L. Chien, Phys. Rev. Lett. **86**, 5585 (2001).
[24]J. Geerk, X. X. Xi, and G. Linker, Zeitschrift fur Physik B **73**, 329 (1988).
[25]A. G. Sun, L. M. Paulius, D. A. Gajewski, M. B. Maple, and R. C. Dynes, Phys. Rev. B **50**, 3266 (1994).
[26]J. Y. T. Wei, N.-C. Yeh, D. F. Garrigus, and M. Strasik, Phys. Rev. Lett. **81**, 2542 (1998).
[27]G. Deutscher, Rev. Mod. Phys. **77**, 109 (2005).
[28]G. Wexler, Proc. Phys. Soc. **89**, 927 (1966).
[29]P. Chalsani, S. K. Upadhyay, O. Ozatay, and R. A. Buhrman, Phys. Rev. B **75**, 094417 (2007).
[30]B. Nadgorny, *Handbook of Spin Transport and Magnetism* (Taylor and Francis, New York, 2011), p. 531.